

New Procedure for Estimation of Power Fundamental Phasor Parameters in Presence of Decaying DC Components

DIMITRIJE ROZGIĆ, PREDRAG B. PETROVIĆ
Faculty of Technical Sciences Čačak, University of Kragujevac,
Svetog Save 65, 32000 Čačak,
SERBIA

Abstract: - The paper proposes a new algorithm for the estimation of the fundamental phasor in a power system, based on the removal of exponentially decaying DC components (DDCs). These components, as well as high-order harmonics and noise components, have a considerable effect on accuracy and speed of convergence in numerical and digital relays – speed of the protection relay operation. A Discrete Fourier Transform (DFT) based approach with a modified Prony method was used to calculate and remove the unwanted effect of DDCs in a time interval slightly longer than the period of the fundamental harmonics. The proposed procedure offers the possibility to estimate the parameters of unwanted DDCs in a simpler and analytically more precise way, thus facilitating its program implementation. The algorithm offers the ability to easily adjust the response speed - detection time. This flexibility of the algorithm provides a compromise in terms of response speed as well as expected reliability and security of fault detection. The developed procedure enables the monitoring of the very demanding dynamics of the current signal in short-circuit conditions, and thus the estimation of the phasor parameters of the energy signal so that the relay protection can respond to this emergency in the most adequate (adaptive) way - it becomes more precise and faster in its response. The algorithm has low numerical and computational complexity while maintaining its high performance even in conditions of a very strong noise signal. The simulation results for different test signals demonstrate high precision in the estimation of the fundamental phasor of the proposed algorithm.

Key-Words: - Phasor estimation, Fault current, DFT, Prony, DDCs, Digital protection.

Received: June 25, 2021. Revised: July 13, 2022. Accepted: September 12, 2022. Published: October 6, 2022.

1 Introduction

In the event of a fault situation in the power system, DDCs are superimposed on the already existing sinusoidal components in the current signal, which significantly degrades the desired waveform of the processed quantities. Current transformers - CTS - measure the flow of current through the power system lines. During a fault, the fault output current signal from the CT also has two exponentially DDCs, while in the input CT current there is only one exponentially DDC [1]. Exponentially DDCs are non-periodic signals and their frequency spectrum covers all frequencies, for which reason these components greatly affect the accuracy and speed of convergence of the procedure in which phasor estimation is performed, i.e. they tend to lead to inevitable error in estimation [2]. Thus this component decreases the accuracy and speed of the protection relay operation, with the DDC magnitude and duration being dependent upon the time constant of the transient circuit, as well as the grid voltage at the transient beginning. For these reasons, the current exponentially DDCs must be taken into

account when calculating the phasor of the basic frequency component of the relay signal.

Over the last few decades, several techniques and algorithms have been proposed to reduce or eliminate the harmful effect in the processing of current signals, occurring as a consequence of the present DDCs. In the paper [2] by using FCDFT (Full Cycle DFT), the processed signal is decomposed into two PS (partial sum)-even and odd indices. By subtracting the sum of the odd indices from the sum of the even indices, an error in the calculated fundamental harmonic phasor can be determined, which is a consequence of the present DDCs. In [3], three consecutive real parts of phasors obtained using FCDFT are used for the estimation of DDCs. The estimated exponential part is subtracted from the input signal samples, thereby eliminating the error which occurred as a consequence of the present DDCs, and also eliminating all DDCs approximated with only a single DDC. The procedure requires $N+2$ samples of the processed signal, where N samples cover the entire period of the processed signal.

In [4], a general modification of the conventional DFT-based algorithm is proposed, so that the alternate application of the FCDFT and HCDFT algorithms is enabled. The key idea is based on the fact that by combining two consecutive real and imaginary filter outputs, the complete elimination of the side effect that occurs due to the presence of exponentially DDCs can be performed, with variable sampling strategies in the phasor measurement process. The procedure described in [5] demonstrated the estimation of the two DDCs using the Prony method in a combination with a sinusoidal filter (imaginary part of the FCDFT), followed by an FIR Notch filter which removes the fundamental harmonic component. The Prony method is effective in a situation where the estimation of exponential components from a set of equidistant signal samples is performed over a signal that is not loaded by a noise component. The noise in the input signal limits the application of such an algorithm, which the authors explicitly state in their work and for what reason they propose a different approach. The second algorithm proposed in [5] is based on the application of FCDFT/HCDFT, using a second-order FIR Notch filter to achieve the elimination of multiple DDCs. Initial filtering eliminates harmonics of the order $N/4$, using two additional samples, to reduce the numerical complexity of the Notch filter and to minimize the time for the realization. Finally, using the FCDFT we come to a position to determine the phasor of order $N/4$. It has been theoretically shown that multiple DDCs can be combined into a single DDC using the proposed approach.

As a consequence of the application of a low-pass first-order filter, new DDCs with a known time constant are generated in several algorithms. If the low-pass filter is of the second order, two DDCs with known time constants are generated in the signal. On this basis, in [6], four consecutive phasors are obtained using the FCDFT technique and a first-order low-pass filter, while five consecutive phasors are obtained using FCDFT and a second-order low-pass filter. In [7], the DDCs are approximated by a straight line or a square polynomial. The direction coefficients of a line are determined over the partial sum (PS) of even and odd indices or as the best uniform approximation of the exponential function by a straight line. The performance of the algorithm degrades in a situation when the values of the time constants are small (high dynamics of these components). The algorithms [2-7] are sensitive to the presence of noise in the processed input current signal.

The paper [8] proposes a method based on FCDFT with three additional samples to identify two DDCs based on Prony analysis. This identification is performed on two types of FCDFT coefficients - at the quarter and half sampling frequencies to reduce the sensitivity of Prony analysis to noise, and also to increase the estimation speed. [9] presents a DC offset removal algorithm to improve the fault location, voltage, and current phasor estimates, using the RMS-wavelet and non-linear least squares methods - LES.

The authors of [10] propose a new hybrid method for the determination of the amplitude of DC and the value of its corresponding time constant by applying the Hilbert transformation and integrating the fault current signal within one cycle.

Furthermore, [11] describes a modified method realized by combining integrations and HCDFT, which accurately estimates the original value of the fundamental phasor in the half-cycle, taking into account the presence of harmonics in the waveforms of the processed signal. The same authors in [12] utilize frequency modulation and Prony complex theory to estimate the unknown characteristics of DDCs. In [13], the error due to the DC offset in the phasor value obtained from DFT is calculated and eliminated with the auto-regressive (AR) model. A fundamental phasor estimation algorithm based on the application of a completely new complex filter is presented in [14], the zeros of which are adjusted to achieve suppression of DDCs. The poles of the filter must be specified in such a way as to compensate for the phase-shifting effect of the zeros. In [15], a new adaptive structure is proposed with Volterra (Volterrea filter) expansions of input samples to estimate harmonic and sequence components simultaneously within the three-phase power system. The new structure is a compromise between LMS (Least Mean Square) and LMF (Least Mean Fourth) which is modeled as LMS/F (Least Mean Square/Fourth) having a modified cost function (to improve the error convergence properties). The LES-based distance relaying method proposed in [16] offers improvements in the estimation procedure by adjusting the length of the estimation window and raising the sampling rate. The article [17] presents the design of a new digital filter, C-Charm DF (Cleaned Characteristic Harmonic Digital Filter) for the estimation of noisy transient signals with decreasing exponential components, harmonics, and interharmonics. The proposed filter is focused on the estimation of the components of a transient signal in the field of fault detection and location.

The paper proposes a completely new approach - an algorithm for the processing of a complex current signal in the presence of several DDCs. The algorithm developed in this paper is based on the minimization of the mean square error between the actual and the assumed waveform of the signal, whereby the signal received at the output of the sinusoidal filter is estimated. This filter eliminates higher harmonic components and maps multiple DDCs (reducing their magnitudes and maintaining the value of time constants) with attenuation of the present noise signal. The proposed approach offers correction of DFT results due to incompleteness of the number of samples in the processed signal period, which is a particularly expressed problem in modern commercially available numerical relays. The processed current signal is released by multiple DDCs, for which the relevant operation of the relay protection system is achieved, allows adjustment of its reaction speed, and provides greater reliability, sensitivity, and security, as well as better selectivity of the numerical relay. All these benefits make the proposed algorithm suitable for practical application in protective devices in modern power systems.

The algorithm is based on a modification of the DFT-Prony method, which provides an opportunity to reduce the number of unknowns of the corresponding polynomial for the estimation of the unknown DDCs. Unlike [5], the problem that arises by applying the Prony method is solved here, so that all present DDCs that occur at the output of the sine filter are replaced by one exponential DDC, which makes the Prony method immune to the present noise. In this way, new analytical expressions are derived which define the values of the parameters of unwanted components in the current signal that is the subject of processing, without the need to calculate inverse matrices. At the cost of reduced estimation speed, greater accuracy and robustness have been achieved compared to previously known estimation procedures. The developed method is extremely resistant to the presence of noise signal and frequency mismatch, enabling easy program implementation and requiring samples from time intervals slightly longer than a single period of the fundamental current phasor. The proposed estimation procedure corrects the error inherent in the application of the DFT algorithm in estimating the fundamental harmonic phasor as a consequence of realistically present DDCs in the fault current. DDCs, as well as noise, cause oscillations - deviations in the estimation results when applying the DFT algorithm, which certainly affects the timely activation of the protection relay, especially the distance protection. Distance protection can

react to a fault outside the protected zone (overreach), which reduces the security of fault detection, while in a situation where it does not react to a fault within the protected zone (under-reach) there is a decrease in dependability in the detection process of fault places. Through the development of the proposed procedure, the authors have insisted on increasing the dependability and security in the process of fault detection, considering that by reducing the oscillations in the response in estimating the amplitude and phase of the basic phasor, i.e. with faster convergence towards the actual value of the estimated parameters, we enable the relay to adequately react to the detected fault current in a shorter time interval with greater dependability, thereby effectively preventing the impact current from jeopardizing the utility grid. In this way, more reliable operation of modern numerical relays is enabled, which is confirmed both through the presented simulation checks and through comparison with relevant procedures from the available literature.

2 Proposed DC Offset Estimation Algorithm

In general, when a fault occurs in a power system, DDCs are added to the current waveform and the sampled faulted current signal can be expressed as follows [5]

$$i[n] = A_0 + \sum_{j=1}^{N/2-1} A_j \cos\left(\frac{2\pi j}{N}n + \varphi_j\right) + \sum_{m=1}^3 D_m e^{-\frac{nT_s}{\tau_m}} + e(n) \quad (1)$$

where A_0 is the DC bias, D_m and τ_m are the magnitudes and the time constant of an exponential component ($m=1$ for the primary, $m=2$ for the secondary and $m=3$ for auxiliary DDCs in the current signals of CT), respectively; A_j and φ_j are the amplitude and the phase angle of the j -th harmonic component, respectively; T_s is the sampling interval; $e(n)$ is additive white noise, and N is the number of samples per cycle. In the above representation, we assume that sinusoidal components with frequencies higher than the $(N/2-1)$ order are eliminated by an anti-aliasing low-pass filter, by the Nyquist sampling criterion. This model includes the most complex possible content of the signal that is the subject of processing, in contrast to the model that is the subject of consideration in [18], and which is limited to only one DDC and odd multiple harmonics.

Since FCDFT is immune to harmonics and DC bias [5, 7], the phasor of the fundamental frequency component is calculated as

$$I_{RF} = \frac{2}{N} \sum_{n=0}^{N-1} i[n] \cos\left(\frac{2\pi}{N} n\right) \quad (2)$$

$$I_{IF} = \frac{2}{N} \sum_{n=0}^{N-1} i[n] \sin\left(\frac{2\pi}{N} n\right)$$

where I_{RF} and I_{IF} are the real and imaginary parts of the fundamental frequency phasor, respectively. By moving the data window, i.e. by shifting it for an arbitrary number of samples, it is possible to form a series of the real and imaginary parts of the fundamental phasor defined above

$$I_{RF}(k) = \frac{2}{N} \sum_{n=0}^{N-1} i[n+k] \cos\left(\frac{2\pi}{N} n\right) \quad (3)$$

$$I_{IF}(k) = \frac{2}{N} \sum_{n=0}^{N-1} i[n+k] \sin\left(\frac{2\pi}{N} n\right), k = 0, 1, 2, \dots, M$$

where $3 \leq M \leq N/4$ (M is the whole number). For a higher value of k , the proposed algorithms become more immune to the present noise component (at the cost of shifting the data window), i.e. slower estimations. After we include (1) in (3), we get

$$I_{RF}(k) = A_1 \cos\left(\frac{2\pi}{N} k + \varphi_1\right) + D_{RF1} e^{-\frac{kT_s}{\tau_1}} + D_{RF2} e^{-\frac{kT_s}{\tau_2}} + D_{RF3} e^{-\frac{kT_s}{\tau_3}} + e_1(k) \quad (4)$$

where A_1 and φ_1 are magnitudes and phases of the fundamental phasor, D_{RF1} , D_{RF2} , D_{RF3} , τ_1 , τ_2 , and τ_3 are magnitudes of the real parts of DDCs and their corresponding time constants, while $e_1(k)$ is the part of the additive white noise after the signal defined with (1) was filtered.

2.1 Equivalent Representation of Multiple DDCs

The actual value of the real part of the fundamental frequency phasor can be approximated-modeled with

$$I_{RF}^{apr}(k) = A_1 \cos\left(\frac{2\pi}{N} k + \varphi_1\right) + I_{RF}^D(k) = A_1 \cos\left(\frac{2\pi}{N} k + \varphi_1\right) + D_{RF} e^{-\frac{kT_s}{\tau}} \quad (5)$$

where $I_{RF}^D(k)$ is that component of the real part of the phasor that arises as a consequence of all existing DDCs? In a way analogous to the procedure used for the real part of the fundamental phasor, its imaginary part can be defined as

$$I_{IF}(k) = y_k = -A_1 \sin\left(\frac{2\pi}{N} k + \varphi_1\right) + D_{IF1} e^{-\frac{kT_s}{\tau_1}} + D_{IF2} e^{-\frac{kT_s}{\tau_2}} + D_{IF3} e^{-\frac{kT_s}{\tau_3}} + e_2(k) \quad (6)$$

where y_k is the imaginary part of the samples of the processed input signal after the sine filter has been applied ($e_2(k)$ is the part of the additive white noise after this filtering). As in (5), we will model this part of the phasor with

$$\hat{y}_k = I_{IF}^{apr}(k) = -A_1 \sin\left(\frac{2\pi}{N} k + \varphi_1\right) + I_{IF}^D(k) = A_1 \sin\left(\frac{2\pi}{N} k + \varphi_1\right) + D_{IF} e^{-\frac{kT_s}{\tau}} \quad (7)$$

where $I_{IF}^D(k)$ is that component of the imaginary part of the phasor that arises as a consequence of all DDCs? The first members in relations (4) and (6) are the result of the orthogonality of trigonometric functions in the expressions defined in (3).

The $D_{RF} e^{-\frac{kT_s}{\tau}}$ in (5) is a unique DDC of the real part of the phasor with a unique time constant t and magnitude D_{RF} (this analogously applies in equation (7), where D_{IF} is the magnitude of the unique DDC of the imaginary part of the phasor), obtained after using in (4) an approximation of two or more DDCs by one such component

$$D_{RF1} e^{-\frac{kT_s}{\tau_1}} + D_{RF2} e^{-\frac{kT_s}{\tau_2}} + \dots \approx D_{RF} e^{-\frac{kT_s}{\tau}} \quad (8)$$

to enable the later application of the Prony method of estimating the parameters of the fundamental phasor. Namely, the Prony method can be applied to a signal of the forms (4) and (6), with multiple DDCs – however, such an algorithm would be practically unusable in the conditions of noise present in the processed signal, since the Prony method is extremely sensitive to noise. It is well known that a greater correlation between the actual values of the signal that is the subject of processing and the assumed mathematical model is achieved by its extension. The authors approached the approximation of shapes (5) and (7), where the unknown parameters will be determined by the method of least squares, thus minimizing the error between the actual and the assumed (mathematical) signal model. The time constant and magnitude of the equivalent DDC do not depend on the sample index. The estimation problem defined in this way is nonlinear, and the resulting system to be solved is a predetermined system of nonlinear equations. For this reason, the application of the Prony method has become extremely effective, with much better performance than can be achieved with for example the well-known Newton-Raphson method. Additionally, this approximation significantly reduces the number of required arithmetic operations (basic operations only). Mathematically speaking, this approximation is completely correct, the new basis functions are $\sin x$, $\cos x$, and e^x and they form a linearly independent set of functions and thus can be the basis of vector space. The approximation of multiple DDCs in [2, 5] is performed in a point, while in [4] the approximation in the next point is performed based on the value of the time constant from the previous point.

Furthermore, while in the algorithm proposed here the approximation is performed based on the values taken at the interval, the number of measurements required to calculate the unknown signal parameters (5) and (7) is less than $N/4$. This allowed the authors to better track the dynamics of DDCs and increase the resistance to the present noise component (interval averaging).

Based on this approximation (equation (8)) we can conclude that

$$\begin{aligned} I_{RF}^D(k) &= \frac{2}{N} \sum_{n=0}^{N-1} D e^{-\frac{(n+k)T_s}{\tau}} \cos\left(\frac{2\pi}{N}n\right); \\ I_{IF}^D(k) &= \frac{2}{N} \sum_{n=0}^{N-1} D e^{-\frac{(n+k)T_s}{\tau}} \sin\left(\frac{2\pi}{N}n\right) \end{aligned} \quad (9)$$

where D is the magnitude of the unique DDC of the signal defined by (1) before the input current signal is passed through the sine and cosine filters. This parameter is needed to establish a relationship between the magnitude of the real and imaginary parts of DDCs, and as such does not have to be determined analytically. It follows that it is

$$I_{RF}^D(k) + jI_{IF}^D(k) = \frac{2}{N} \sum_{n=0}^{N-1} D e^{-\frac{(n+k)T_s}{\tau}} e^{j\frac{2\pi}{N}n} = \frac{2}{N} D e^{-\frac{kT_s}{\tau}} \sum_{n=0}^{N-1} \left(e^{j\frac{2\pi}{N} - \frac{T_s}{\tau}} \right)^n \quad (10)$$

where the following applies

$$\begin{aligned} \sum_{n=0}^{N-1} e^{\left(j\frac{2\pi}{N} - \frac{T_s}{\tau} \right)n} &= \frac{e^{-N\frac{T_s}{\tau}} - 1}{e^{-\frac{T_s}{\tau}} e^{j\frac{2\pi}{N}} - 1} \\ &= \frac{\left(e^{-N\frac{T_s}{\tau}} - 1 \right) \left(e^{-\frac{T_s}{\tau}} e^{-j\frac{2\pi}{N}} - 1 \right)}{e^{-\frac{2T_s}{\tau}} - e^{-\frac{T_s}{\tau}} \left(e^{j\frac{2\pi}{N}} + e^{-j\frac{2\pi}{N}} \right) + 1} = \frac{\left(e^{-N\frac{T_s}{\tau}} - 1 \right) \left(e^{-\frac{T_s}{\tau}} e^{-j\frac{2\pi}{N}} - 1 \right)}{e^{-\frac{2T_s}{\tau}} - 2e^{-\frac{T_s}{\tau}} \cos\frac{2\pi}{N} + 1} \end{aligned} \quad (11)$$

It follows that we can define it D_{RF} as

$$D_{RF} = \frac{2}{N} D (E^N - 1) \frac{E \cos\frac{2\pi}{N} - 1}{E^2 - 2E \cos\frac{2\pi}{N} + 1}; E = e^{-\frac{T_s}{\tau}} \quad (12)$$

and D_{IF} as

$$D_{IF} = \frac{2}{N} D (E^N - 1) \frac{-E \sin\frac{2\pi}{N}}{E^2 - 2E \cos\frac{2\pi}{N} + 1} \quad (13)$$

The accuracy of the proposed estimation procedure is certainly affected by the fact whether complete synchronization with the carrier frequency has been performed, since it varies in real conditions, leading to the truncation error. To completely overcome this problem, it would be necessary to initially determine the frequency of the carrier signal, for which the procedure [19] could be

used, based on the advanced zero-crossing technique, which makes the proposed procedure adaptive in this regard. Most modern protection devices align the sampling frequency with the fundamental frequency of the power system so that it can eliminate truncation errors. In the simulation analysis, the magnitude of the estimation error due to frequency mismatch will be estimated. The basis of the developed algorithm is the non-recursive DFT method. It is well known that DFT is robust to the possible presence of higher harmonic components if the sampling frequency is aligned with the carrier frequency. Therefore, the carrier-fundamental frequency must be continuously estimated and the sampling frequency adjusted, which is done in the proposed algorithms. In that way, the presence of higher harmonics will not affect the accuracy and precision of the output results of estimating the parameters of the fundamental phasor.

2.2 Prony-based Approach

The Prony method approximates a series of equidistant signal samples by the sum of complex exponential functions. The procedure is suitable when there are decreasing one-way components or attenuated harmonic components in the signal [20]. The Prony method can be applied to a signal of the form (5) or (7). When testing the algorithm, it turns out that it is less sensitive to noise if the Prony method is applied to the signal obtained by a sine filter (7). Using the least squares method, we will minimize the error between the actual (6) and the assumed (mathematical) model of the signal (7), whereby we calculate the unknown parameters from the predetermined system of equations

$$\begin{aligned} -A_1 \sin\varphi_1 + D_{IF} &= y_0 \\ -A_1 \sin\left(\frac{2\pi}{N} + \varphi_1\right) + D_{IF} E &= y_1 \\ &\vdots \\ -A_1 \sin\left(\frac{2\pi}{N} M + \varphi_1\right) + D_{IF} E^M &= y_M \end{aligned} \quad (14)$$

The system of equations (14) is nonlinear and its approximate solution will be determined by the Prony method. Using Euler's formula

$$\sin x = \frac{e^{jx} - e^{-jx}}{2j} \quad (15)$$

the system (14) can be written as

$$\begin{aligned} \underline{B}_1 + \underline{B}_2 + \underline{B}_3 &= y_0 \\ \underline{B}_1 \underline{z}_1 + \underline{B}_2 \underline{z}_2 + \underline{B}_3 \underline{z}_3 &= y_1 \\ &\vdots \\ \underline{B}_1 \underline{z}_1^M + \underline{B}_2 \underline{z}_2^M + \underline{B}_3 \underline{z}_3^M &= y_M \end{aligned} \quad (16)$$

where

$$\underline{B}_1 = j \cdot \frac{A_1}{2} e^{j\varphi_1}; \underline{B}_2 = -j \cdot \frac{A_1}{2} e^{-j\varphi_1}; \underline{B}_3 = D_{IF}; \underline{z}_1 = e^{j\frac{2\pi}{N}}; \underline{z}_2 = e^{-j\frac{2\pi}{N}}; \underline{z}_3 = E \quad (17)$$

Using the proposed approach we come to the position to reduce the number of unknowns in the corresponding polynomial. The goal of applying the Prony method is to determine an unknown parameter $\underline{z}_3 = E$. (16) can be rewritten in the matrix form

$$\underline{\mathbf{Z}} \cdot \underline{\mathbf{B}} = \underline{\mathbf{Y}} \quad (18)$$

where

$$\underline{\mathbf{Z}} = \begin{pmatrix} 1 & 1 & 1 \\ \underline{z}_1 & \underline{z}_2 & \underline{z}_3 \\ \vdots & \vdots & \vdots \\ \underline{z}_1^M & \underline{z}_2^M & \underline{z}_3^M \end{pmatrix}, \underline{\mathbf{B}} = \begin{pmatrix} \underline{B}_1 \\ \underline{B}_2 \\ \underline{B}_3 \end{pmatrix}, \underline{\mathbf{Y}} = \begin{pmatrix} y_0 \\ y_1 \\ \vdots \\ y_M \end{pmatrix} \quad (19)$$

The first step in the Prony method implies forming a polynomial

$$P(\underline{z}) = (\underline{z} - \underline{z}_1) \cdot (\underline{z} - \underline{z}_2) (\underline{z} - \underline{z}_3) \quad (20)$$

Using the basic principle of algebra, we obtain a third-order polynomial with the roots $\underline{z}_1, \underline{z}_2, \underline{z}_3$, which can be written in a slightly modified form

$$P(\underline{z}) = \underline{z}^3 + a_2 \underline{z}^2 + a_1 \underline{z} + a_0 \quad (21)$$

As $P(\underline{z}_i) = 0$ for $i=1, 2, 3$, it follows that

$$\begin{aligned} a_2 &= -(\underline{z}_1 + \underline{z}_2 + \underline{z}_3) = -2 \cos \frac{2\pi}{N} - E \\ a_1 &= \underline{z}_1 \underline{z}_2 + \underline{z}_1 \underline{z}_3 + \underline{z}_2 \underline{z}_3 = 2E \cos \frac{2\pi}{N} + 1 \\ a_0 &= -\underline{z}_1 \underline{z}_2 \underline{z}_3 = -E \end{aligned} \quad (22)$$

The next step in the Prony method is the formation of the vectors $\underline{\mathbf{H}}_k$ -(auxiliary vectors of the Prony method)

$$\begin{aligned} \underline{\mathbf{H}}_1 &= (a_0, a_1, a_2, 1, 0, 0, \dots, 0)_{1 \times (M+1)} \\ \underline{\mathbf{H}}_2 &= (0, a_0, a_1, a_2, 1, 0, \dots, 0)_{1 \times (M+1)} \\ &\vdots \\ \underline{\mathbf{H}}_{M-2} &= (0, \dots, 0, a_0, a_1, a_2, 1)_{1 \times (M+1)} \end{aligned} \quad (23)$$

Multiplying the matrix $\underline{\mathbf{Z}}$ with vectors $\underline{\mathbf{H}}_k$ we obtain

$$\underline{\mathbf{H}}_1 \cdot \underline{\mathbf{Z}} = (a_0, a_1, a_2, 1, 0, 0, \dots, 0) \cdot \begin{pmatrix} 1 & 1 & 1 \\ \underline{z}_1 & \underline{z}_2 & \underline{z}_3 \\ \vdots & \vdots & \vdots \\ \underline{z}_1^M & \underline{z}_2^M & \underline{z}_3^M \end{pmatrix} = (h_{11} \quad h_{12} \quad h_{13}) \quad (24)$$

that is

$$\begin{aligned} h_{11} &= a_0 + a_1 \underline{z}_1 + a_2 \underline{z}_1^2 + \underline{z}_1^3 = P(\underline{z}_1) = 0 \\ h_{12} &= a_0 + a_1 \underline{z}_2 + a_2 \underline{z}_2^2 + \underline{z}_2^3 = P(\underline{z}_2) = 0 \\ h_{13} &= a_0 + a_1 \underline{z}_3 + a_2 \underline{z}_3^2 + \underline{z}_3^3 = P(\underline{z}_3) = 0 \end{aligned} \quad (25)$$

Repeating the same methodology for all other vectors $\underline{\mathbf{H}}_k$ for the last of the vectors $\underline{\mathbf{H}}_k$ can be written as

$$\underline{\mathbf{H}}_{M-2} \cdot \underline{\mathbf{Z}} = (0, \dots, a_0, a_1, a_2, 1) \cdot \begin{pmatrix} 1 & 1 & 1 \\ \underline{z}_1 & \underline{z}_2 & \underline{z}_3 \\ \vdots & \vdots & \vdots \\ \underline{z}_1^M & \underline{z}_2^M & \underline{z}_3^M \end{pmatrix} = (h_{11} \quad h_{12} \quad h_{13}) \quad (26)$$

where the following applies

$$\begin{aligned} h_{11} &= a_0 \underline{z}_1^{M-3} + a_1 \underline{z}_1^{M-2} + a_2 \underline{z}_1^{M-1} + \underline{z}_1^M = \underline{z}_1^{M-3} P(\underline{z}_1) = 0 \\ h_{12} &= a_0 \underline{z}_2^{M-3} + a_1 \underline{z}_2^{M-2} + a_2 \underline{z}_2^{M-1} + \underline{z}_2^M = \underline{z}_2^{M-3} P(\underline{z}_2) = 0 \\ h_{13} &= a_0 \underline{z}_3^{M-3} + a_1 \underline{z}_3^{M-2} + a_2 \underline{z}_3^{M-1} + \underline{z}_3^M = \underline{z}_3^{M-3} P(\underline{z}_3) = 0 \end{aligned} \quad (27)$$

It is practically valid (for a system of equations) that

$$\begin{aligned} \underline{\mathbf{H}}_k \cdot \underline{\mathbf{Z}} &= (0 \quad 0 \quad 0), \quad k = 1, 2, \dots, M-2 \\ \underline{\mathbf{H}}_k \cdot \underline{\mathbf{Z}} \cdot \underline{\mathbf{B}} &= 0 \end{aligned} \quad (28)$$

It follows that

$$\underline{\mathbf{H}}_k \cdot \underline{\mathbf{Y}} = 0, \quad k = 1, 2, \dots, M-2 \quad (29)$$

that is, a predetermined system of linear equations of form is obtained

$$\begin{aligned} a_0 y_0 + a_1 y_1 + a_2 y_2 + y_3 &= 0 \\ a_0 y_1 + a_1 y_2 + a_2 y_3 + y_4 &= 0 \\ &\vdots \\ a_0 y_{M-3} + a_1 y_{M-2} + a_2 y_{M-1} + y_M &= 0 \end{aligned} \quad (30)$$

A system (30), taking the values defined in (22), with the unknown E , can be written as

$$\begin{aligned} E \left(y_0 - 2 \cos \frac{2\pi}{N} y_1 + y_2 \right) &= y_1 - 2 \cos \frac{2\pi}{N} y_2 + y_3 \\ E \left(y_1 - 2 \cos \frac{2\pi}{N} y_2 + y_3 \right) &= y_2 - 2 \cos \frac{2\pi}{N} y_3 + y_4 \\ &\vdots \\ E \left(y_{M-3} - 2 \cos \frac{2\pi}{N} y_{M-2} + y_{M-1} \right) &= y_{M-2} - 2 \cos \frac{2\pi}{N} y_{M-1} + y_M \end{aligned} \quad (31)$$

By solving the system of equations defined above, using the least squares method, a solution to an unknown E is obtained in the form

$$E = \frac{\sum_{i=0}^{M-3} \left(y_i - 2 \cos \frac{2\pi}{N} y_{i+1} + y_{i+2} \right) \left(y_{i+1} - 2 \cos \frac{2\pi}{N} y_{i+2} + y_{i+3} \right)}{\sum_{i=0}^{M-3} \left(y_{i+1} - 2 \cos \frac{2\pi}{N} y_{i+2} + y_{i+3} \right)^2} \quad (32)$$

By a consistent application of Prony's method, i.e. by solving the system (18) by the method of least squares, the phasor of the fundamental harmonic can be determined. This would further computationally burden the algorithm. This step can be bypassed, as it is much easier to determine the components of the real and imaginary parts of the phasor, due to the existence of the DDCs. From (5) and (7), for $k=0, 1$; we obtain

$$\begin{aligned} I_{RF}(0) &= A_1 \cos \varphi_1 + D_{RF} \\ I_{RF}(1) &= A_1 \cos \left(\frac{2\pi}{N} + \varphi_1 \right) + D_{RF} E \\ I_{IF}(0) &= -A_1 \sin \varphi_1 + D_{IF} \\ I_{IF}(1) &= -A_1 \sin \left(\frac{2\pi}{N} + \varphi_1 \right) + D_{IF} E \end{aligned} \quad (33)$$

For the estimation of D_{RF} and D_{IF} , all available information on the measured value of the processed signal can be used (for each $k = 0, 1, \dots, M$); however, this does not increase the robustness of the algorithm to the present noise - it is the calculation of the parameter E in (33) that is most sensitive to noise. Satisfactory accuracy has already been achieved with $k = 0, 1$ (due to the robustness of the used sine and cosine filters to the noise), with a reduction in the number of computational operations in the estimation process. By solving the system of equations (33) we get

$$D_{RF} = \frac{(I_{IF}(1) - E I_{IF}(0)) \sin \frac{2\pi}{N} - (I_{RF}(1) + E I_{RF}(0)) \cos \frac{2\pi}{N} + I_{RF}(0) + E I_{RF}(1)}{E^2 - 2E \cos \frac{2\pi}{N} + 1} \quad (34)$$

Based on (12) and (13) it follows that

$$D_{IF} = -D_{RF} \frac{E \sin \frac{2\pi}{N}}{E \cos \frac{2\pi}{N} - 1} \quad (35)$$

The fundamental harmonic phasor can now be calculated using the following relations

$$\begin{aligned} A_1 &= \sqrt{(I_{RF}(0) - D_{RF})^2 + (I_{IF}(0) - D_{IF})^2} \\ \varphi_1 &= \arctg \frac{-I_{IF}(0) + D_{IF}}{I_{RF}(0) - D_{RF}} \end{aligned} \quad (36)$$

It should be noted that there is only one unknown - E in the predetermined system of equations (31), for which reason at least one equation is needed for it to be calculated. In the conditions of noise present in the processed signal, it is necessary to apply more equations. For example, if we take five equations, M must satisfy the condition that $3 < M \leq 8$, namely, the approximation (8) is sufficiently correct for $M \leq 16$. In this paper, the data window corresponding to the fundamental period of the processed signal is a length of $N=64$, therefore, the approximation (8) is sufficiently accurate for $M \leq N/4$.

The flowchart of the proposed phasor estimation algorithm is shown in Fig. 1. After conditioning the current signal via CT, the processed signal is sampled via a special acquisition card and forms a series of measurements from which all harmonic components of order higher than N are eliminated using a low-pass filter. As mentioned in the text above, using FCDFT, i.e. sine filter, the real and imaginary parts of the processed current phasor are separated. By applying the described modified Prony's procedure, the value of the unknown parameter E is determined, as equality (32). From the real part of the current phasor (estimated by a cosine filter via FCDFT), two consecutive doses of the fundamental harmonic - relation (33) are calculated. Based on the determined value of parameter E and the value of two consecutive measurements from the output of the sine filter, all unknown parameters of the fundamental harmonic of the processed current phasor are determined, which returns us to the beginning of the procedure, which is, we can access the estimation on the next set of data.

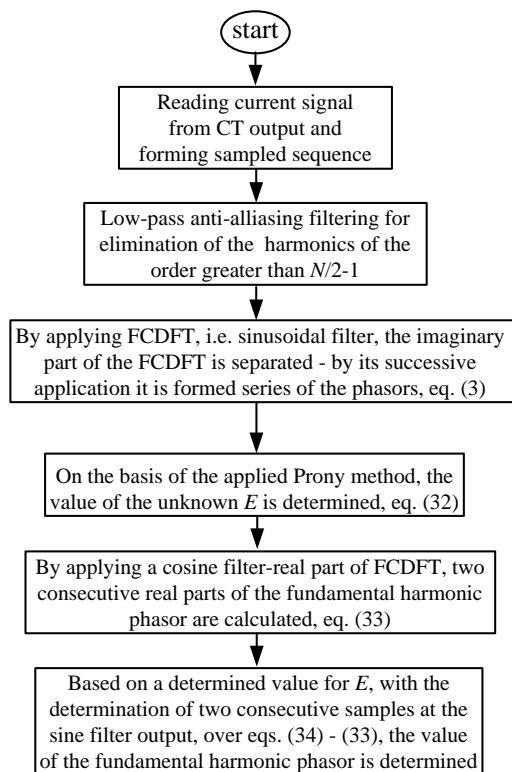


Fig. 1: Proposed phasor estimation procedure

3 Simulation Results

To see as precisely as possible the performance of the algorithm proposed here for the estimation of the fundamental current phasor in the conditions of failure, its simulation check was performed on multiple analytically defined fault current data and a fault transmission line with a CT [5]. Practically the most challenging case studies which can occur in practice are given in this section of the paper. The simulation tests were carried out with Matlab/Simulink and Mathematica. In all tests, the number of samples was $N=64$, although it should be noted that very similar results are obtained with a twice lower number of samples. The carrier frequency of the processed current signal was $f_0=50\text{Hz}$. The number of present DDCs is changed from case to case, as well as the harmonic content of the current signal with a variable SNR (signal to noise ratio). The assessment of the accuracy of the proposed method in the estimation of the fundamental phasor was compared with procedures well-known in the literature for their precision and accuracy.

3.1 Case 1: Fault Current with two DDCs and Noise

To check the performance of the proposed algorithm for estimating the fundamental current phasor under the conditions of both primary and secondary DDCs, the following simulation verification (in the Mathematica program package) is performed on the next two generated signals [5]

$$i_1(t) = \sum_{j=1}^{31} \frac{15}{j^2} (1-h(t-T_f)) \cos j\omega t + \sum_{j=1}^{31} \frac{100}{j^2} h(t-T_f) \cos j\omega(t-T_f) + (37)$$

$$+ 0.9 \sum_{j=1}^{31} \frac{100}{j^2} h(t-T_f) e^{-100(t-T_f)} + 0.1 \sum_{j=1}^{31} \frac{100}{j^2} h(t-T_f) e^{-2.5(t-T_f)} + e(t)$$

$$i_2(t) = \sum_{j=1}^{31} \frac{15}{j^2} (1-h(t-T_f)) \cos j\omega t + \sum_{j=1}^{31} \frac{100}{j^2} h(t-T_f) \cos j\omega(t-T_f) + (38)$$

$$+ 0.9 \sum_{j=1}^{31} \frac{100}{j^2} h(t-T_f) e^{-10(t-T_f)} + 0.1 \sum_{j=1}^{31} \frac{100}{j^2} h(t-T_f) e^{-2.5(t-T_f)} + e(t)$$

with two time constants: primary DDC of $\tau_1=1/100\text{s}$ and $\tau_1=1/10\text{s}$ (for the signal $i_2(t)$) and $\tau_2=1/2.5\text{s}$ for secondary DDC [21].

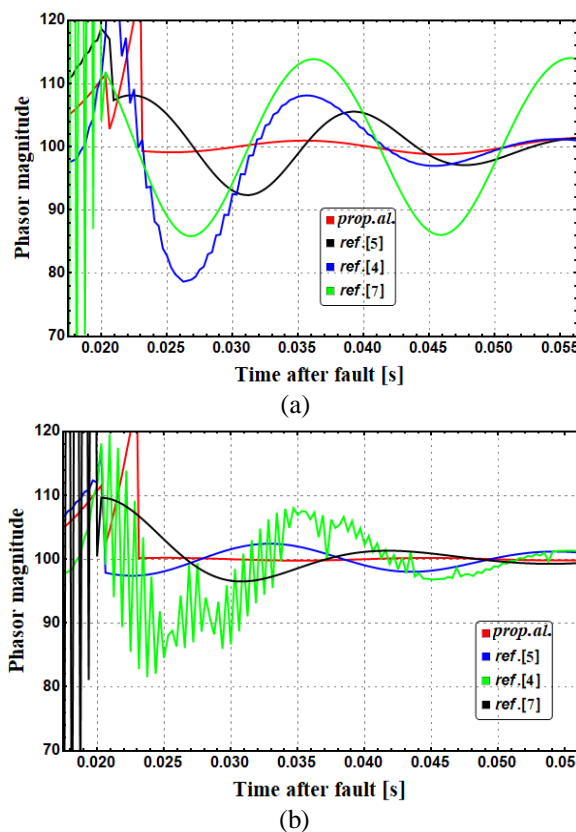


Fig. 2: Time responses of the four methods for $\tau_1=1/100\text{s}$ and different SNR: (a) SNR=30dB; (b) SNR=50dB

The amplitude of the observed primary DDC depends on the fault-inception angle φ_f [5, 7] and the time constant, but in such generated signals we assume that the phase is $\varphi_f=0$, since the highest value of the primary DDC is obtained in this

situation. In the above relations (37)-(38), $h(t)$ is the Heaviside function, $e(t)$ is the additive white noise and T_f is the moment at which the fault occurred - it is assumed that the error occurs at the moment $T_f=0.02s$.

Time responses for the estimation procedure proposed here, as well as for the methods described in [4, 5, 7], are given in Figs. 2 and 3. For the comparison to be completely realistic and correct, the same sampling frequency was used in all algorithms on the test signals used in [5]. In the simulation tests performed here, in contrast to [4, 5, 7], noise signals of higher power and in a wider dynamic range were used. Compared to the method proposed here, algorithms [4, 5, 7] require a smaller number of samples to calculate the unknown parameters of the basic phasor, which in turn provides faster convergence of results with fewer oscillations in response and greater robustness concerning the noise present.

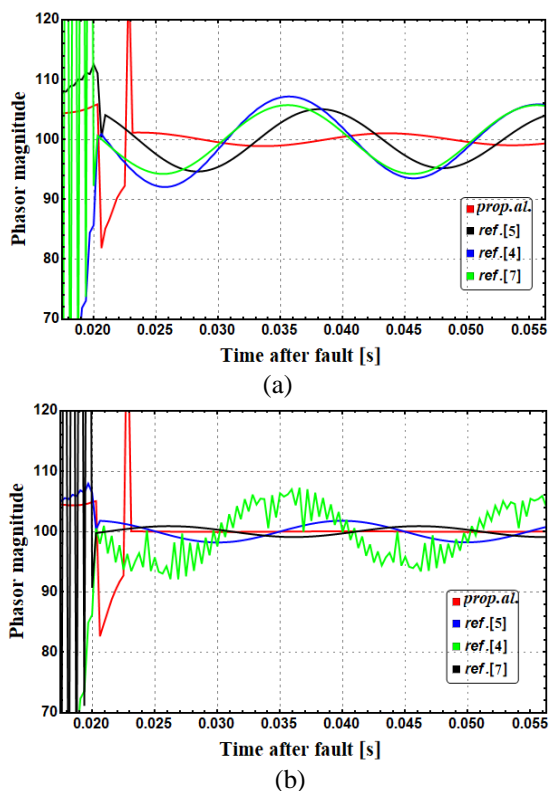


Fig. 3: Time responses of the four for $\tau_I=1/10s$ and for different SNR: (a) SNR=30dB; (b) SNR=50dB

Based on the obtained results, it can be concluded that a satisfactory estimation of phasor value by the proposed algorithm is achieved after a time interval that is slightly longer than the period of the fundamental harmonic of the current signal. As we can see, the oscillations are expressed in the estimation process, which is especially pronounced in a situation where the SNR is small. The

estimation procedure proposed here is much more resistant - robust to the noise present. Its time responses are less fluctuated than methods described in [4, 5, 7, 15]. In addition, the algorithm described in the paper offers the possibility of adjusting the response rate, where the minimum number of samples required for its implementation equals $(N+3) \cdot T_s$. This number of samples is slightly higher than that required by the comparative work - $N \cdot T_s$ [7], $(N+1) \cdot T_s$ [4], $(N+2) \cdot T_s$ [5], so that the reaction rate-speed is almost identical in all the procedures described. However, by extending the execution time to $(N+9) \cdot T_s$, we achieve a significant reduction in oscillations in the output results in presence of a strong noise signal, i.e. faster convergence to real value. The procedures described in [4, 5, 7] insist on a precisely defined number of measurements, which is not the case here, and it is this flexibility of the proposed algorithm that provides a compromise on satisfactory response speed and expected dependability and security in fault detection. Of course, the speed of response cannot be the only criterion that will justify the practical application of an algorithm. In addition to the performance evaluation, the process must take into account dependability, security, sensitivity, and selectivity, which is achieved by the proposed approach. All these criteria are related to the magnitude of the oscillations of the output results, i.e. they are significantly improved by reducing oscillations.

The signal-to-noise ratio (SNR) at the transmission lines is known to be variable and is often much higher than 40 dB [5, 22]. Additive white Gaussian noise was used in the simulation, where the SNR of $i(t)$ is given as the power ratio of the fundamental harmonic (with frequency f_0) component to the white noise.

It can also be concluded that the large value of the time constant of the primary DDC causes somewhat smaller oscillations in the phasor estimation. The proposed method, as well as the modified DFT methods [3, 6], can eliminate the DC offsets, using the data window of one cycle length plus k samples for estimation.

To better understand the performance of the methods compared here in terms of accuracy in estimating the amplitude of the fundamental current phasor, Table 1 lists the mean values and standard deviations for both types of test signals used in the simulation process (signals defined with (37) and (38), taking the first sample at the moment in which fault occurs). Determination of the mean value and standard deviation σ_{A1} in the estimates of the amplitude of the fundamental harmonic was

performed on a sample of 200 simulations, where the exact value of the amplitude was $A_I=100A$.

It can be seen from Table 1 that the proposed algorithm achieves high accuracy in phasor measurement and has a more stable performance than methods described in [4, 5, 7], indicating their immunity to the DC offset.

Table 1. Mean value and standard deviation in the estimation of the amplitude of the fundamental current phasor

Signal		SNR=60dB	SNR=50dB	SNR=40dB	SNR=30dB	
		B	B	B	B	
Prop. algor.	$i_1(t)$	mean	99.9991	100.015	99.9753	99.9138
		stand. dev.	0.057833	0.196029	0.592769	1.85589
	$i_2(t)$	mean	100.01	99.9726	99.988	99.285
		stand. dev.	0.068449	0.19478	0.6880	1.8798
Ref. [5]	$i_1(t)$	mean	99.9569	100.129	100.669	102.42
		stand. dev.	0.330283	1.11917	3.59098	9.85315
	$i_2(t)$	mean	99.9801	99.9431	99.804	100.14
		stand. dev.	0.426967	1.36371	2.8954	3.4421
Ref. [4]	$i_1(t)$	mean	95.2871	95.6963	103.449	114.267
		stand. dev.	0.944776	2.50128	10.575	12.0804
	$i_2(t)$	mean	98.9474	98.7096	99.784 9	100.51
		stand. dev.	0.21658	0.81265	1.9516	1.5647
Ref. [7]	$i_1(t)$	mean	109.696	109.704	109.723	110.394
		stand. dev.	0.0285112	0.0838301	0.294912	1.60331
	$i_2(t)$	mean	99.847	99.8399	99.888	100.63
		stand. dev.	0.034203	0.11394	0.3992	1.4638

3.1.1 Frequency Mismatch

Many measurements in modern power systems, based on digital signal processing, are carried out under the assumption that the system works at the nominal frequency (50 Hz or 60 Hz), that is, a fixed sampling frequency is used, synchronized with the nominal frequency of the system. However, the actual frequency changes over time and deviates from the nominal frequency. The most common reason for frequency deviation is a mismatch between production and consumption. Namely, in the steady state, a balance was achieved between the production of active power on the one hand and the consumption and losses of active power on the other hand. However, the increasing integration of renewable energy sources in power systems, whose power is often uncontrollable (wind power plants, hydropower plants, photovoltaic plants...), makes it challenging to maintain a balance between production and consumption. This imbalance is directly reflected in the frequency of the voltage and

current signals, i.e. the carrier frequency of the system, and leads to a mismatch of the sampling frequency with the system frequency. The mismatch between the sampling frequency and the system frequency (spectral leakage) is a source of errors in phasor estimation algorithms based on the DFT method. The error is small for a small frequency deviation and increases with a larger deviation. In short-circuit conditions, the frequency deviation can lead to a large error in phasor estimation, especially in the presence of DDCs.

In the works with which the comparison was made [4, 5, 7], the authors did not take into account the estimation error due to the variation of the carrier phasor frequency, which is known to exist in the real system and was taken to be $\pm 0.5\text{Hz}$ in the simulation. Table 2 lists the mean values and standard deviations for the test signal (37) for all algorithms in the situation when there is a frequency mismatch, where the results are given for the case when the carrier frequency is 49.5 Hz (first value in the column) and 50.5Hz (value in parentheses).

Table 2. Mean value and standard deviation in the estimation of the amplitude of the fundamental current phasor for signal defined with (37) in the situation when existing frequency mismatch

Proposed algorithm		SNR=60dB	SNR=50dB	SNR=40dB	SNR=30dB
		B	B	B	B
Proposed algorithm	mean	97.654 (100.766)	97.673 (100.762)	97.631 (100.732)	97.55 (100.792)
	stand. dev.	0.0645 (0.0617)	0.202 (0.1728)	0.598 (0.5895)	2.061 (1.816)
Ref. [5]	mean	94.982 (114.814)	94.951 (114.762)	94.8702 (114.862)	102.42 (113.46)
	stand. dev.	0.0823 (0.4104)	0.283 (1.3881)	3.591 (4.51188)	9.853 (10.652)
Ref. [4]	mean	101.672 (134.704)	101.381 (134.037)	100.945 (125.792)	109.637 (119.848)
	stand. dev.	0.581 (0.2445)	2.0539 (1.46279)	5.374 (12.3635)	12.408 (12.9536)
Ref. [7]	mean	108.06 (111.579)	108.049 (111.581)	108.157 (111.63)	108.864 (112.121)
	stand. dev.	0.043 (0.01356)	0.133 (0.04049)	0.444 (0.159)	1.844 (0.7985)

From the obtained results, it can be concluded that the proposed algorithm is more robust compared to the methods described in [4, 5, 7]. Furthermore, stable response in presence of decaying DC offset and also off-nominal frequency condition is another capability of the proposed approach.

3.2 Case 2: Fault Current with Different Relative Amplitude of DDCs

In the order to further evaluate the performances of the proposed estimation procedure, simulation tests are performed for the different relative amplitude of

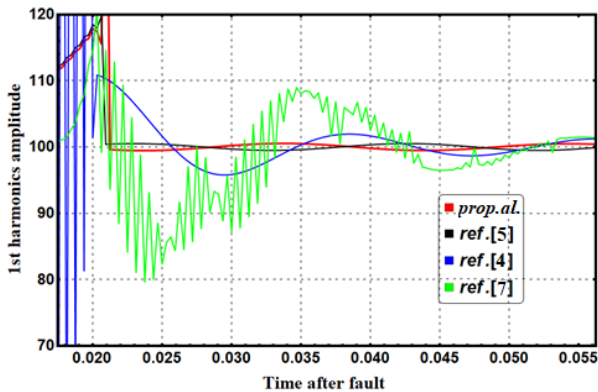
DDCs to the fundamental component and the presence of additive noise for different SNRs (SNR=30dB and SNR=50dB) and the different number of samples $N+M$. The generated signal was defined as

$$i_i(t) = \sum_{j=1}^{31} \frac{15}{j^2} (1-h(t-T_{fj})) \cos j\omega t + \sum_{j=1}^{31} \frac{100}{j^2} h(t-T_{fj}) \cos j\omega(t-T_j) + \quad (39)$$

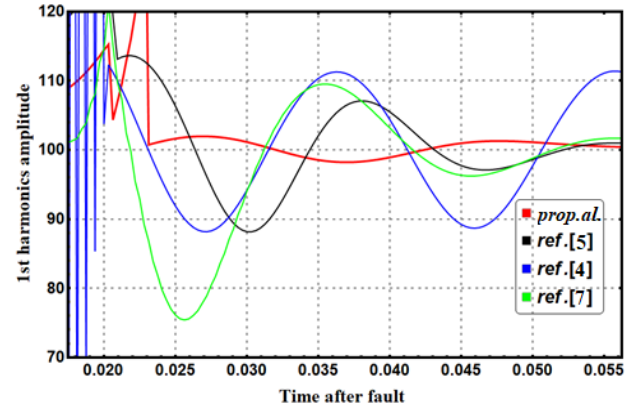
$$+ K_i \cdot \sum_{j=1}^{31} \frac{100}{j^2} h(t-T_{fj}) e^{-\frac{(t-T_{fj})}{\tau_1}} + 0.1 \cdot K_i \cdot \sum_{j=1}^{31} \frac{100}{j^2} h(t-T_j) e^{-\frac{(t-T_j)}{\tau_2}} + e(t), \quad i=1, \dots, 4$$

where K_i defines the relative amplitude of the DDCs amplitude: $K_1=1$; $K_2=0.707$; $K_3=0.5$; $K_4=0.1$. The time constant of DDCs is settled as $\tau_1=1/100$ s (10ms) and $\tau_2=1/400$ s (2.5ms) – we observe the cases with demanding dynamics (smaller value of the first time constant). Time responses for the proposed algorithm, as well as for the methods described in [4, 5, 7], are given in Figs. 4 and 5.

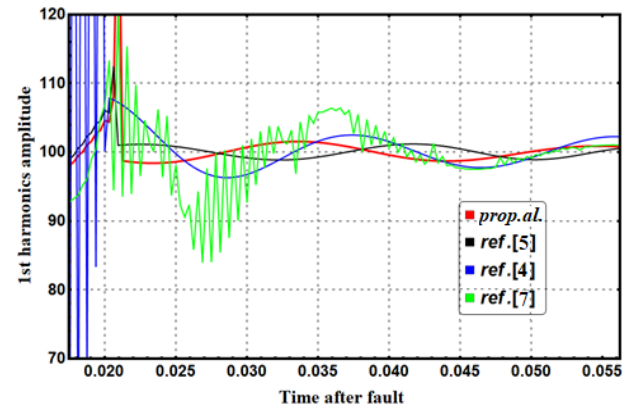
For the simulation check in Fig. 4, we use the test signal defined with equation (39), having two DDCs, while in the case of simulation presented in Fig. 5, we use signal (39) without a second DDC – only DDC with time constant τ_1 , neglecting the second DDC with the time constant τ_2 . As in Case 1, the proposed estimation procedure possesses higher accuracy in phasor measurement and has a more stable performance than the methods described in [4, 5, 7]. It should be especially emphasized that in situations when the level of the present noise signal is high, SNR = 50, for a small $M=3$, an extremely fast estimation of the values of the fundamental harmonic phasor is allowed by the proposed procedure.



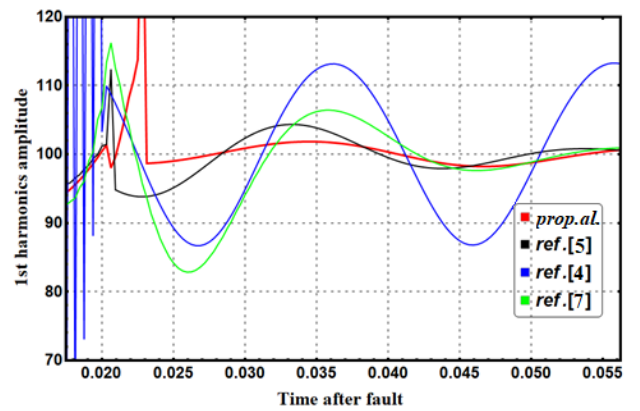
(a)



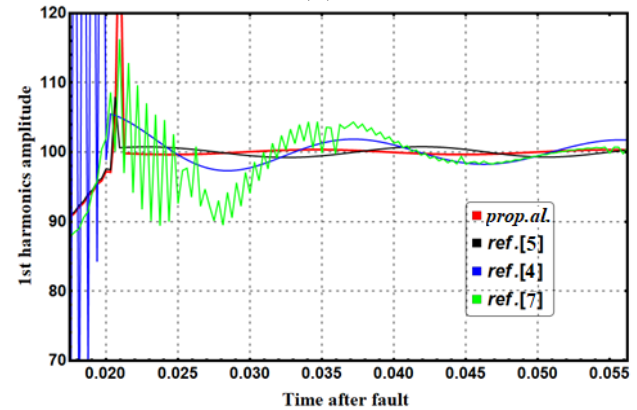
(b)



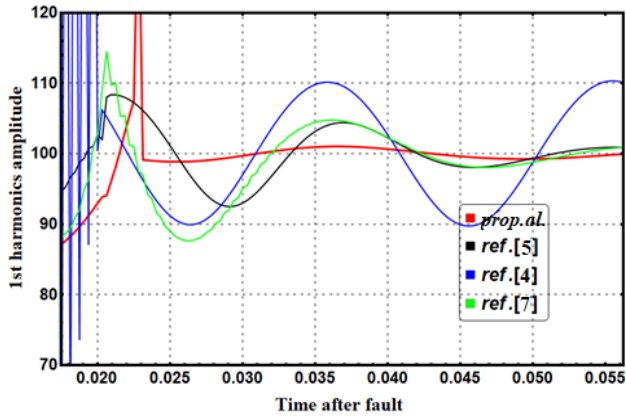
(c)



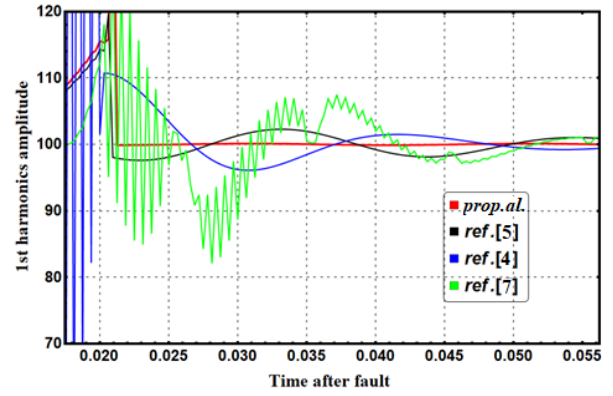
(d)



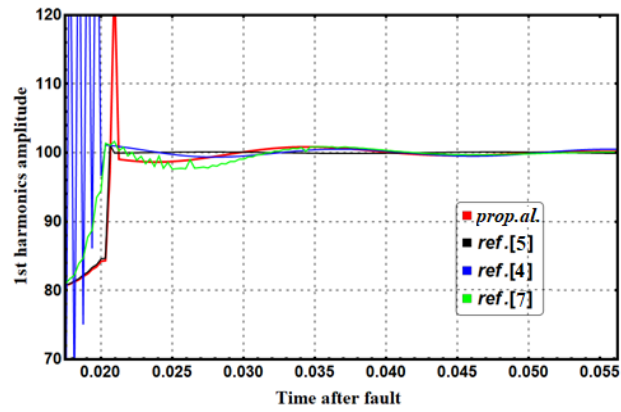
(e)



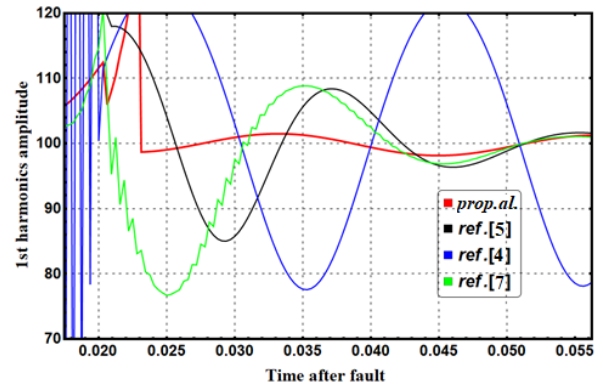
(f)



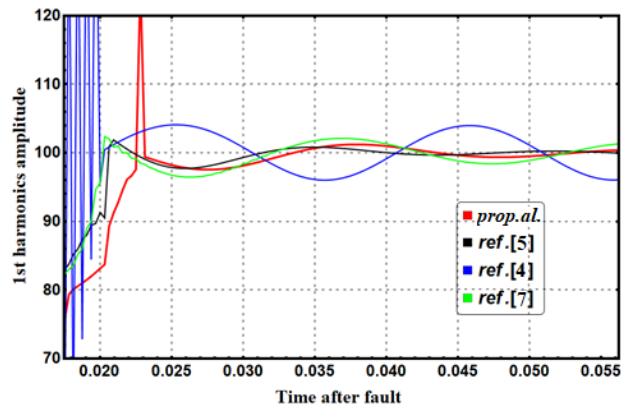
(a)



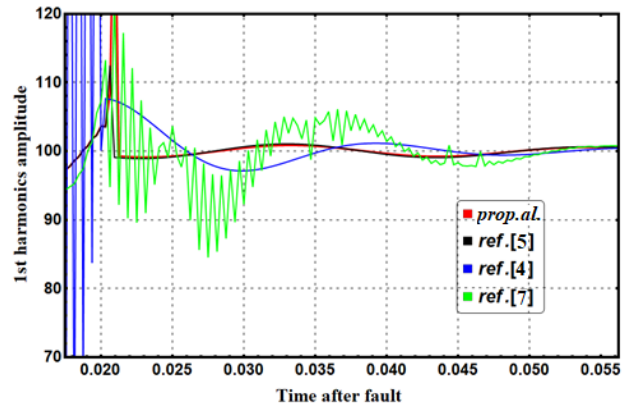
(g)



(b)

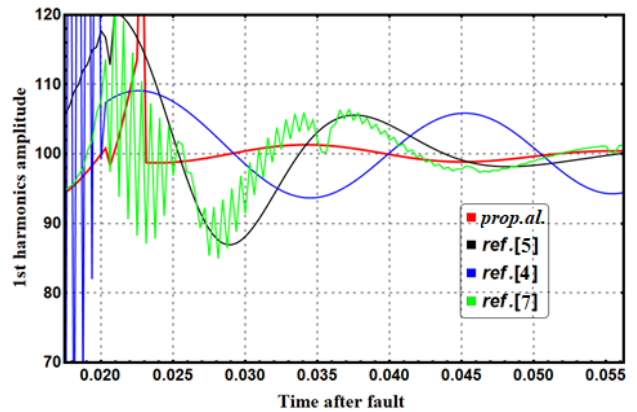


(h)



(c)

Fig. 4: Time responses of the four methods for the signal defined in (39) and for (a) K_1 , SNR=50dB, $M=3$; (b) K_1 , SNR=30dB, $M=9$; (c) K_2 , SNR=50dB, $M=3$; (d) K_2 , SNR=30dB, $M=9$; (e) K_3 , SNR=50dB, $M=3$; (f) K_3 , SNR=30dB, $M=9$; (g) K_4 , SNR=50dB, $M=3$; (h) K_4 , SNR=30dB, $M=9$



(d)

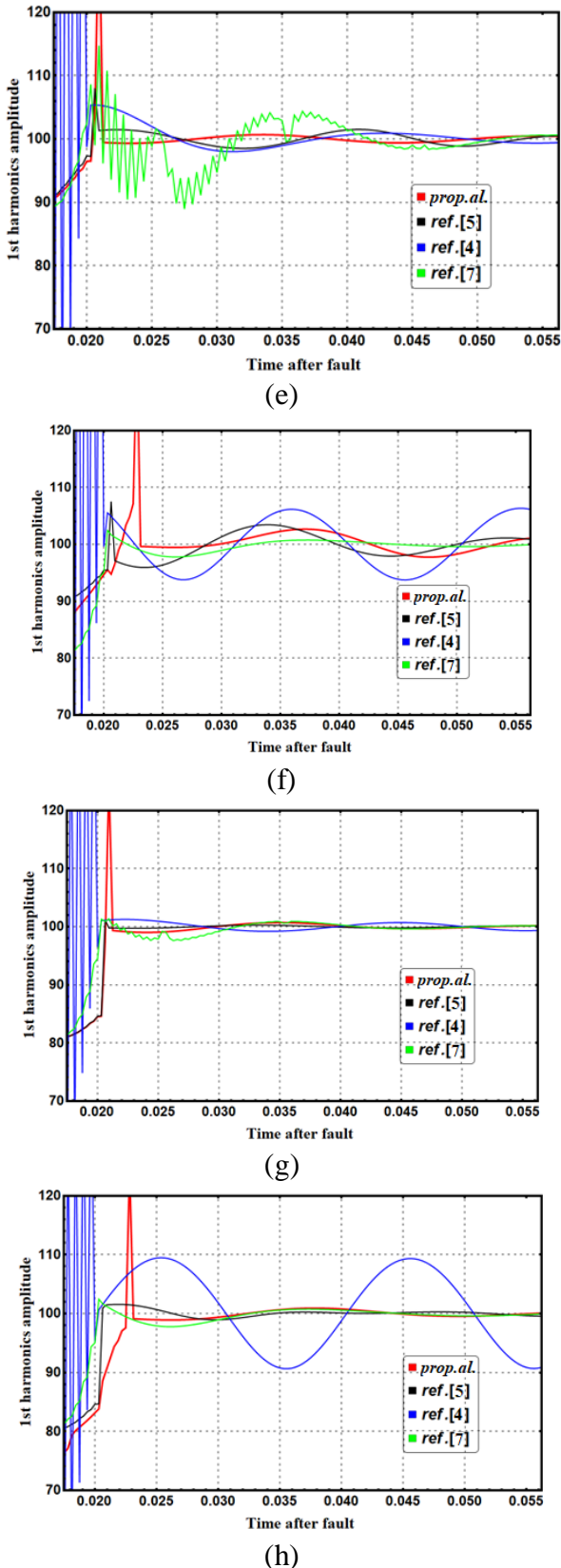


Fig. 5: Time responses of the four methods in the situation where in signal defined with (39) there exists only first DDC with time constant τ_1 and for (a) K_1 , SNR=50dB, $M=3$; (b) K_1 , SNR=30dB, $M=9$; (c) K_2 , SNR=50dB, $M=3$; (d) K_2 , SNR=30dB, $M=9$;

(e) K_3 , SNR=50dB, $M=3$; (f) K_3 , SNR=30dB, $M=9$;
(g) K_4 , SNR=50dB, $M=3$; (h) K_4 , SNR=30dB, $M=9$

3.3 Case 3: Fault Current with Mutually Opposite DDCs

In real power systems, the occurrence of the difference between the sign of two exponentially decaying terms is possible. This indicates that CT secondary responds towards opposing exponential decay of primary current (note that primary current is not affected) [23]. Also, a negative sign associated with the second DDC indicates that the primary power circuit tries to maintain instantaneous current at the time of fault inception. To check the performance of the proposed algorithm in this condition we use the following test signal for evaluation

$$i_i(t) = \sum_{j=1}^{31} \frac{15}{j^2} (1 - h(t - T_f)) \cos j\omega t + \sum_{j=1}^{31} \frac{100}{j^2} h(t - T_f) \cos j\omega(t - T_f) + \quad (40)$$

$$+ K_i \cdot \sum_{j=1}^{31} \frac{100}{j^2} h(t - T_f) e^{-\frac{(t-T_f)}{\tau_1}} - \frac{\tau_1}{\tau_2} \cdot K_i \cdot \sum_{j=1}^{31} \frac{100}{j^2} h(t - T_f) e^{-\frac{(t-T_f)}{\tau_2}} + e(t), \quad i = 1, \dots, 4$$

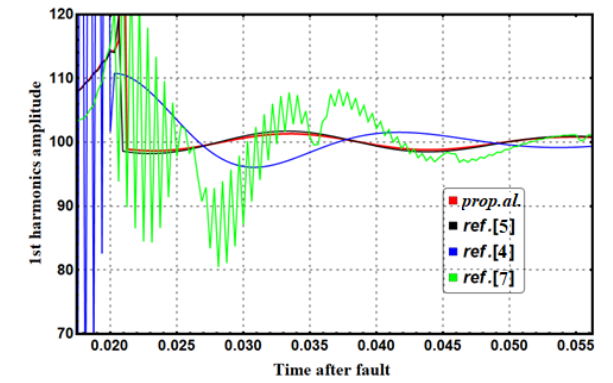
where the meanings of the parameters are the same as in equation (39). Time responses for the proposed procedure, as well as for the algorithms used for comparison and described in [4, 5, 7] are given in Figs. 6.

In the above-observed conditions where DDCs are mutually opposite, the proposed estimation procedure can provide accurate and fast estimation, with much less oscillation in response to the methods with which the comparison was performed.

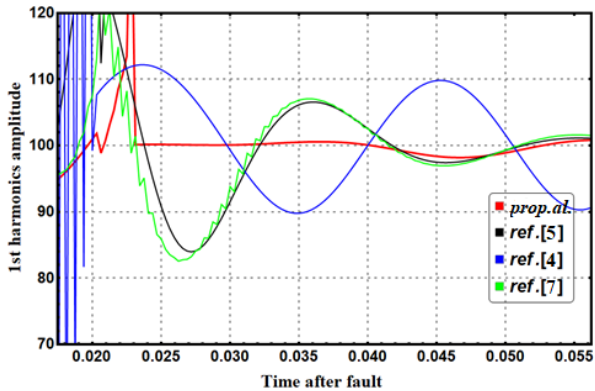
3.4 Faulted Transmission Line

The method proposed in this paper was evaluated using MATLAB Simulink for several fault scenarios on the 345-kV transmission line with a length of 50 km, based on the model of a simple power system shown in Fig. 7, to compare their efficiency and precision in the estimation of the fundamental phasor to the conventional [4, 5, 7] solutions. The parameters of the network are given in Table 3 [2, 5]. During normal operating conditions, the voltage and current signals are close to pure sine waveforms of the nominal frequency. However, when faults and disturbances occur in power systems, many transient components are generated and the nominal frequency current and/or voltage signals are distorted. These components include decaying DC

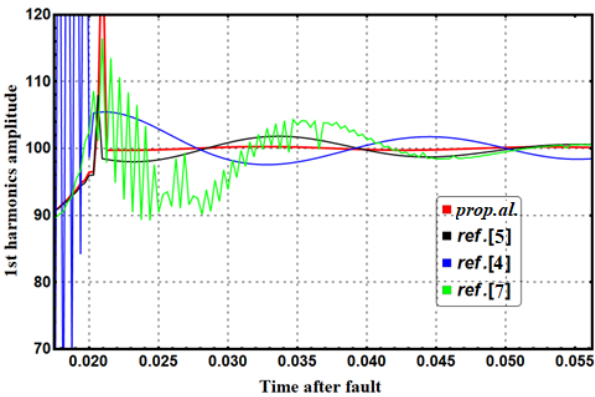
offset, harmonics, and off-nominal frequency components.



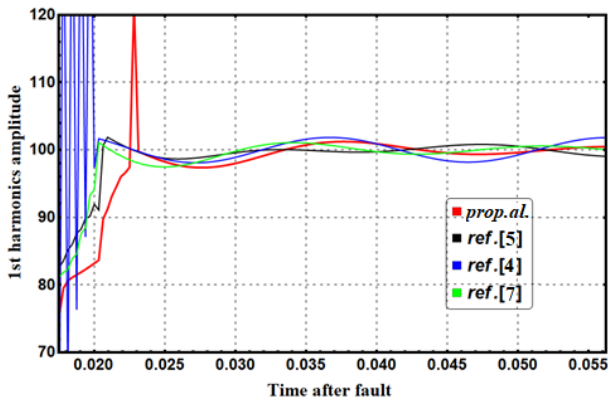
(a)



(b)



(c)



(d)

Fig. 6: Time responses of the four methods for the signal defined in (40) and for (a) K_1 , SNR=50dB, $M=3$; (b) K_2 , SNR=30dB, $M=9$; (c) K_3 , SNR=50dB, $M=3$; (d) K_4 , SNR=30dB, $M=9$

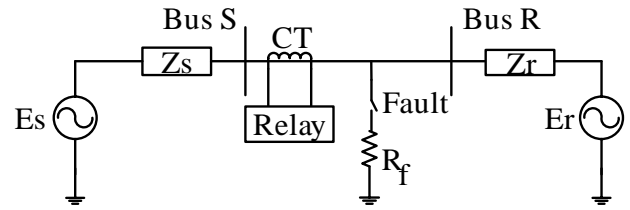


Fig. 7: Power system with the single line used for simulation

A current signal is acquired at Bus S, Fig. 8 - phase-A current sequences for the 0.1- Ω and 10- Ω fault resistances, using a CT circuit which is described in [24], formed using a C400 (2000:5) CT and a 1 Ω resistive load [5]. This circuit was also described and realized in MATLAB/Simulink (Current Saturation Transformer-power_ctest.mdl) [5, 25].

The simulation check was performed under the assumption that a single-phase short-circuit fault occurs 20 km from the BUS S (the phase-A-to-ground fault), for two different fault resistances of 0.1 Ω and 10 Ω , while the fault occurs at $t=0$ s. Butterworth's second-order analog low-pass filter with a cut-off frequency of 600 Hz was used to eliminate unwanted higher-order harmonic components, i.e. for anti-aliasing. In all of the performed tests, the sampling rate was set to 64 samples/cycle. As can be seen in Fig. 9, the results obtained by applying the estimation procedure proposed here reach (converge to) the desired value after the time interval slightly longer than the duration of one cycle (23.1 ms for the proposed algorithms) after the failure has occurred. The used analog anti-aliasing filter introduces an additional time delay in the estimation of the fundamental phasor.

Table 3. Transmission Line Parameters

	Parameter	Value	Unit
Positive & Negative	r		
	R_1, R_2	0.0345	Ω/km
	L_1, L_2	0.9724	mH/km
	C_1, C_2	0.0117	pF/km
Zero	R_o	0.2511	Ω/km
	L_o	2.7058	mH/km
	C_o	0.0045	pF/km

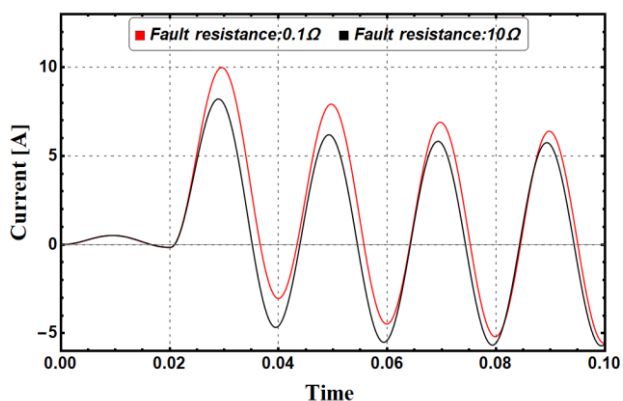
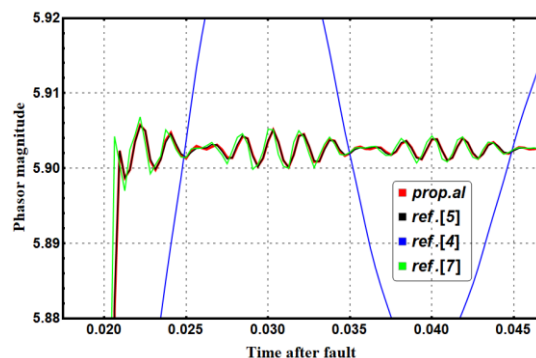


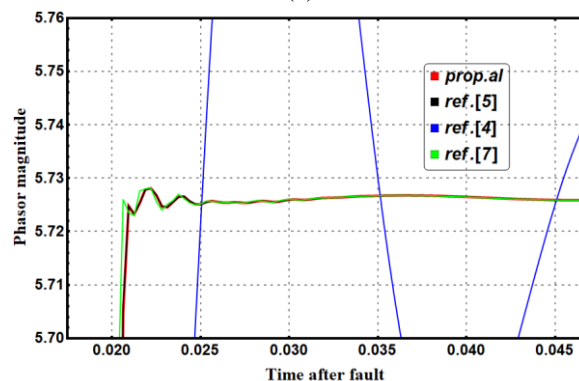
Fig. 8: Waveforms of simulated fault currents in the phase-A transmission

Based on the time responses for the estimation method proposed here, shown in Fig. 9, it can be seen that it shows a better performance compared to [4, 5, 7]. In the case where the fault resistance is $0.1\ \Omega$, Fig. 9(a), the proposed method is shown to cause significantly less fluctuation in response, while the methods [4, 7] are sensitive to the presence of secondary DDC of CT. These fluctuations are even more pronounced if the fault resistance is $10\ \Omega$. For these reasons, the proposed algorithm can be successfully applied in practice in a situation where it is a faulted transmission line, which has a greater fault resistance. Namely, transmission lines possess a lower level of noise and higher harmonics, and for these reasons, the response speed of the proposed algorithm can be set to $(N+3)T_s$, which is the time approximately equal to the time required for execution in [4, 5, 7].

The proposed algorithm, contrary to the PS-DFT (Partial Sums based DFT) [7], data windowing [26], conventional DFT method [27], LES-based procedure [16], C-Charm DF digital filtering algorithm [17] and AI (applied integration) method [28], can remove the DDCs component created by CT. These DDCs have a significant effect on the result of PS-DFT and AI methods, which causes more instability in the obtained results. Also, the proposed method had a better speed of convergence and precision in comparison with the existing conventional DFT-based methods and hybrid approach proposed in [10].



(a)



(b)

Fig. 9: Transient (time) responses of the proposed method under a realistic fault current signal: (a) for fault resistance of $0.1\ \Omega$; (b) for fault resistance of $10\ \Omega$

Through simulation tests, the algorithm confirmed the possibility of achieving a compromise between response speed, computational complexity, and precision. The results of the conducted tests showed that the proposed algorithm achieves better accuracy, has less oscillation of the output results, and faster convergence towards the correct value compared to the algorithms in the works published so far. This is especially pronounced in conditions when the processed signal contains a very strong noise component. The algorithm can adjust the response speed: if the relay is intended for installation in the transmission network, where there is a lower level of noise and higher harmonics, the response speed can be set to $(N+3)T_s$, which is the time approximately equal to the time required for execution until now known algorithms. If the relay is intended for installation in a distribution network, where there is a higher level of noise and higher harmonics, the response time can be set to $(N+10)T_s$, which is an essential comparative advantage of the proposed algorithm. With a small extension of the response time, the oscillations in the estimated parameters are significantly reduced, which ensures greater reliability, sensitivity, and safety, as well as better selectivity of the numerical

relay. All these advantages make the proposed algorithm suitable for practical application in protective devices in power systems.

4 Conclusion

In this paper, a new method for estimating the fundamental current phasor has been proposed, which is based on the modified FCDFT/Prony approach. The proposed algorithms have faster convergence and better precision than the present methods. In addition, during harmonic distortion and also frequency fluctuation, they provide a correct and reliable response. The algorithm is proposed to compromise between the computational burden, accuracy, and speed, thereby reducing the effect of noise in phasor estimation. The results of the conducted simulation tests showed that the proposed method offers greater accuracy in the estimation of the fundamental phasor than the procedures described so far for the same purpose, and is known to produce unwanted oscillations, especially in conditions of a very strong noise signal. The time required for such a process is practically almost equal to the periods of the fundamental harmonic of the current signal that is the subject of processing- the method is suitable to be applied in measurement and protection devices in real power systems. The proposed estimation procedure is based on the application of innovative analytical formulas, which makes the calculation of the unknown parameters mathematically much simpler and more precise. The applicability of the proposed algorithm was confirmed through the simulation of a faulted transmission line using a CT, with much lower oscillation and fluctuation in response than the methods used for comparison.

References:

- [1] S. H. Horowitz and A.G. Phadke, *Power system relaying*, vol. 22, John Wiley & Sons, 2008.
- [2] S. Kang, D. Lee, S. Nam, P. A. Crossley, and Y. Kang, "Fourier Transform-Based Modified Phasor Estimation Method Immune to the Effect of the DC Offsets", *IEEE Transactions on Power Delivery*, 2009, vol. 24, no. 3, pp. 1104-1111.
- [3] J. C. Gu and S.L. Yu, "Removal of DC offset in current and voltage signals using a novel Fourier filter algorithm", *IEEE Transactions on Power Delivery*, 2000, vol.15, no. 1, pp. 73-79.
- [4] K.M. Silva and F.A.O. Nascimento, "Modified DFT-Based Phasor Estimation Algorithms for Numerical Relaying Applications", *IEEE Transactions on Power Delivery*, 2018, vol. 33, no. 3, pp. 1165-1173.
- [5] J.K. Hwang, C.K. Song, and M. G. Jeong, "DFT-Based Phasor Estimation for Removal of the Effect of Multiple DC Components", *IEEE Transactions on Power Delivery*, 2018, vol. 33, no. 6, pp. 2901-2909.
- [6] S. L. Yu and J.C. Gu, "Removal of decaying DC in current and voltage signals using a modified Fourier filter algorithm", *IEEE Transactions on Power Delivery*, 2001, vol. 16, no. 3, pp. 372-379.
- [7] Y. Guo, M. Kezunovic, and D. Chen, "Simplified algorithms for removal of the effect of exponentially decaying DC-offset on the Fourier algorithm", *IEEE Transactions on Power Delivery*, 2003, vol. 18, no. 3, pp. 711-717.
- [8] J. K. Hwang, "Improvement of Phasor Estimation Accuracy by Prony-based Identification of Two Decaying DC Components", *2019 IEEE Power & Energy Society General Meeting (PESGM)*, Atlanta, GA, USA, 2019, pp. 1-5.
- [9] K. W. Min and S. Santoso, "DC Offset Removal Algorithm for Improving Location Estimates of Momentary Faults", *IEEE Transactions on Smart Grid*, 2018, vol. 9, no. 6, pp. 5503-5511.
- [10] M. Tajdinian, M. Z. Jahromi, K. Mohseni, and S. M. Kouhsari, "An analytical approach for removal of decaying DC component considering frequency deviation", *Electric Power Systems Research*, 2016, vol. 130, pp. 208-219.
- [11] M. Tajdinian, A.R. Seifi, and M. Allahbakhshi, "Half-cycle method for exponentially DC components elimination applicable in phasor estimation", *IET Science, Measurement & Technology*, 2017, vol. 11, no. 8, pp. 1032-1042.
- [12] M. Allahbakhshi, M. Tajdinian, A.R. Seifi, J.M Zareian, and A. Bagheri, "Hybrid approach for immunization of DFT-based phasor estimation method against decaying DC components", *IET Science, Measurement & Technology*, 2019, vol 13, no. 2, pp. 238-246.
- [13] W.J. Kim and S.H. Kang, "A DC offset removal algorithm based on AR model", *Journal of International Council on Electrical Engineering*, 2018, vol. 8, no. 1, pp. 156-162.

- [14] B. Jafarpisheh, S. M. Madani, and F. Parvaresh, "Phasor Estimation Algorithm Based on Complex Frequency Filters for Digital Relaying", *IEEE Transactions on Instrumentation and Measurement*, 2018, vol. 67, no. 3, pp. 582-592.
- [15] U. Subudhi, H. K. Sahoo, and S. K. Mishra, "Harmonics and Decaying DC Estimation Using Volterra LMS/F Algorithm", *IEEE Transactions on Industry Applications*, 2018, vol. 54, no. 2, pp. 1108-1118.
- [16] L. Shenji, J. Xingxing, and G. Ramakrishna, "High-speed distance relaying using least error squares method and testing with FPGA", *IET Generation, Transmission & Distribution*, 2019, vol. 13, no. 16, pp. 3591-3600.
- [17] J. Vazquez, J. F. Miñambres, M. A. Zorroza, and J. Lázaro, "Phasor Estimation of Transient Electrical Signals Composed of Harmonics and Interharmonics", *Energies*, 2021, vol. 14, no. 16: 5166. doi:10.3390/en14165166
- [18] L. Xiong, X. Liu, and Y. Liu, "Decaying DC and Harmonic Components Detection for Absorbing Impact Load Currents in Weak Grids", *IEEE Trans. Power Deliv.*, 2021, vol. 36, no. 3, pp. 1907-1910.
- [19] P. B. Petrović and D. Rozgić, "Computational Effective Modified Newton-Raphson Algorithm for Power Harmonics Parameters Estimation", *IET Signal Processing*, 2018, vol. 12, no. 5, pp. 590 – 598.
- [20] J. F. Hauer, C. J. Demeure, and L. L. Scharf, "Initial results in Prony analysis of power system response signals", *IEEE Trans. Power Syst.*, 1990, vol. 5, pp. 80-89.
- [21] G. Benmouyal, "Removal of DC-offset in current waveforms using digital mimic filtering", *IEEE Transactions on Power Delivery*, 1995, vol. 10, no. 2, pp. 621-630.
- [22] J. K. Hwang and Y. Liu, "Noise analysis of power system frequency estimated from angle difference of discrete Fourier transform coefficient", *IEEE Trans. Power Del.*, 2014, vol. 29, no. 4, pp. 1533-1541.
- [23] P. D. Achlerkar and B. K. Panigrahi, "Assessment of DC offset in fault current signal for accurate phasor estimation considering current transformer response", *IET Science, Measurement & Technology*, 2019, vol. 13, no. 3, pp. 403-408.
- [24] D. A. Bradley, C. B. Gray, and D. O'Kelly, "Transient compensation of current transformers". *IEEE Trans. Power App. Syst.*, 1978, vol. PAS-97, no. 4, pp. 1264-1271.
- [25] *Power System Blockset User's Guide*. Natick, MA: the Mathwork, Inc., 2002.
- [26] H. Sardari, B. Mozafari, and H. Shayanfar, "Fast DC Offset Removal for Accurate Phasor Estimation using Half-Cycle Data Window", *Journal of Electrical and Computer Engineering Innovations*, 2021, doi:10.22061/jecei.2021.8205.492
- [27] A.G. Phadke and J.S. Thorp, *Computer Relaying for Power Systems*, Wiley, New York, NY, 2009.
- [28] Y.-S. Cho, C.-K. Lee, G. Jang, and H.J. Lee, "An innovative decaying DC component estimation algorithm for digital relaying", *IEEE Transactions on Power Delivery*, 2009, vol. 24, no. 1, pp. 73-78.

Creative Commons Attribution License 4.0 (Attribution 4.0 International, CC BY 4.0)

This article is published under the terms of the Creative Commons Attribution License 4.0

https://creativecommons.org/licenses/by/4.0/deed.en_US